IOP Publishing Journal of Optics
J. Opt. **13** (2011) 125705 (11pp) doi:10.1088/2040-8978/13/12/125705

Adjustable-focus lenses based on the Alvarez principle

S Barbero[1] **and J Rubinstein**[2]

[1] Instituto de Optica (CSIC), Serrano 121, Madrid 28006, Spain
[2] Department of Mathematics, Technion, Haifa 32000, Israel

E-mail: sergio.barbero@csic.es

Received 17 August 2011, accepted for publication 27 October 2011
Published 1 December 2011
Online at stacks.iop.org/JOpt/13/125705

Abstract
We present a comprehensive approach for the design of adjustable-focus lenses based on the Alvarez principle. The design methodology consists of dividing the lens into two parts: the inner, optical part, where the optical quality is optimized, and the outer, mechanical part, connecting the optical part to the frame. For the optical part, we present a complete optical design methodology to minimize common optical aberrations, considered in ophthalmic lens design, for different focus adjustments. For the mechanical part, we show how to extend the lens surfaces to connect the optical zone with the frame, such that the entire surface is smooth and has acceptable thickness.

Keywords: Alvarez lenses, ophthalmic lens design, adjustable-focus lenses

1. Introduction

In 1967 Alvarez invented [1] a new type of lenses with varifocal properties, intended to be used as spectacle lenses for presbyopia correction. Similar lenses were proposed independently by Lohmann [2]. Two lenses of this type provide an optical power change when one of them is laterally shifted with respect to the other. We shall denote these lenses Alvarez lenses.

As far as we know, no spectacles based on the Alvarez patent for treatment of presbyopia were ever built and commercialized. This is probably due to manufacturing issues, and also because the optical quality of the specific model proposed by Alvarez [1] was not good enough, in particular in comparison with modern designs of progressive addition lenses (PALs).

However, in recent years there has been new interest in using such lenses as adjustable-focus spectacle lenses for developing countries. The World Health Organization estimates that about 150 million people are visually impaired because of myopia, hypermetropia or astigmatism [3], and eight million of these are considered blind. Also, a recent study, based on population-based surveys, estimates that more than one billion people are affected by presbyopia, with more than half of them without any type of visual correction for it [4].

The lack of refractive error correction in these people is due to the unaffordable economical cost and inaccessibility to refraction and spectacle lens dispensing services. Spectacles with self-adjusting refractive power offers a low-cost and adaptable technology for refractive error measurement and correction. Indeed the Alvarez lenses provide a good option for such a technology.

We comment that several spectacle models have been developed and manufactured, or are currently under development, based on the Alvarez concept for the general purpose of providing affordable refraction correction for people in developing countries. Further information on the status of these models can be found on their web pages [5–7]. However, no public information is available about the optical design of the lenses, though some groups have patented their frame mechanical designs [8, 9].

To develop self-adjustable lenses based on the Alvarez principle one needs to solve three main problems. First, one should design one pair of lenses per eye with good optical quality at different relative shift positions, so a person can adjust the pair to achieve optimal power. Then, one should design a frame with appropriate mechanical properties to allow for a convenient and stable shifting of the lenses. The third problem that we must overcome relates to the special geometry of the lenses. As will be explained below, the Alvarez lenses suffer from an inherent problem: their thickness grows rapidly when one moves away from the optical center. Since some of the lens parameters are optically constrained, and since

aesthetic and mechanical issues pose limits on the frame design, one must overcome the rapid growth in thickness by means of a special design of the peripheral part of the lenses.

In summary, a global design of the spectacle lenses comprises three design objectives: the optical part of the lenses, the frame, and the design of the peripheral part of the lenses, where the optical zone of the lenses is extended to meet the constraints imposed by the frame. The goal of this paper is to present methods to deal with the first and the third design objectives. An approach for the second objective (frame design) was previously considered by us [10].

A complete and novel optical design methodology is presented in section 2 (first design objective). This section also includes the analysis of a few theoretical issues related to Alvarez lenses. In section 3 we present an example of application of the optical design methodology. In section 4 we propose a way to design the mechanical (peripheral) zone of the lens (third design objective). Finally, in section 5, some general issues are discussed.

Before proceeding we make two comments on our terminology. First, we use here the notion of astigmatism in the sense in which is used in the optometric community; namely, the astigmatism, or cylinder, is the difference between the two principal powers of the lens. Second, Alvarez-type spectacles contain two lenses per eye. We sometimes refer to the entire optical element consisting of the two lenses as a lens. The interpretation of this expression as the combined effect of two lenses is obvious from the context.

2. Optical design of Alvarez-type spectacle lenses

The key idea of Alvarez [1] was to consider a refractive surface of the form

$$u(x, y) = A(x^3/3 + xy^2) + Bx^2 + Cxy + Dx + F(y). \quad (1)$$

Here (x, y) denote coordinates in the plane, with (0, 0) being the optical center of the lens. The most relevant component of this equation is $A(x^3/3 + xy^2)$, which represents the so-called 'monkey saddle' surface. This surface contains an umbilical point at the central point (0, 0).

A horizontal shift by δ changes the surface to first order by

$$\delta A(x^2 + y^2). \quad (2)$$

This explains, at least to first order, why a horizontal shift varies the power of the lens. We term a surface like u an Alvarez surface. Therefore the quantity A is a measure of the power change that we gain by shifting the lens horizontally by δ. The monkey saddle surface reveals the thickness problem, since the cubic term grows rapidly when we move away from (0, 0).

An actual design is more complicated than the simple monkey saddle surface. At the very least, one should consider lenses comprising one arbitrary surface and another surface that is cubic with respect to one of the coordinates. We use a more general type of surfaces that take the form [11]

$$u(x, y) = \frac{cr^2}{1 + \sqrt{1 - (K + 1)cr^2}} + p_1x^3 + p_2yx^2 + p_3xy^2 + p_4y^3 + p_5xy + p_6x + p_7y. \quad (3)$$

Here $r = \sqrt{x^2 + y^2}$, and c and K are the radius of curvature and the asphericity of the base conic. We define two lenses; each of them has one surface described by equation (3) and the other is a plane, such that the planar surfaces are in contact. The horizontal movement is achieved by sliding the planar surfaces of the lenses with respect to each other. One reason for using an Alvarez-type surface in both lenses is that if the frame's mechanics allows for a maximal shift by δ, then a shift of both lenses by δ in opposite directions gives a relative shift of 2δ. This doubles the dynamical range of the entire spectacle.

Alvarez [1] already proposed to include the linear term (p_6 or p_7 depending on the direction of the lateral shift) to control the lens thickness. Besides this reason we also used this term to control the overall optical quality of the lenses. However, a relevant novelty of our design methodology is that we optimize the nine parameters (the c, K and p_i) of each surface independently. This provides more degrees of freedom for the search for optimal solutions.

2.1. Optical quality analysis

In ophthalmic lens design the shape of the lens surfaces is designed to improve the optical quality for different gaze directions. It is customary to assume that the pupil size is small compared with the area of the lenses and object field-of-view angles, so the main aberrations to be corrected are oblique astigmatism and power error [12]. The other aberration that could be relevant is transverse chromatic aberration [13], which is mainly controlled with proper material selection, so it will not be studied in this work.

The common method to compute the actual power and astigmatism distribution across the lens [14] is shown schematically in figure 1. First, a ray is traced from the center of rotation of the eye (normally modeled to be located 27 mm behind the lens), through the lens, to a far object point (O in figure 1) on the other side of the lens. Then, one computes the refraction by the lens of a small pencil of rays, or a small piece of a wavefront, as they propagate from that object point toward the eye [14]. There are a number of ways to trace this pencil of rays, or small wavefront. For instance, in the case of wavefront tracing, Coddington equations are conventionally applied to compute wavefront refraction at the interface surfaces [15]. However, in the case of highly non-spherical surfaces, such as Alvarez surfaces, more complicated formulas must be applied [16–19]. Another option [14] is to trace a small pencil of rays around each base ray, and then to compute the power and astigmatism from the associated phase function at the image plane (Γ in figure 1). This calculation is repeated for many viewing directions, thus generating a power and astigmatism distribution for the lens system.

2.2. Power variation

As we stated above, Alvarez invented the surface profile of his lens for the purpose of achieving varying optical power upon shifting it with respect to a reference surface. However, even a single stationary Alvarez lens has an interesting property: its paraxial power varies linearly [20]. This makes it a suitable

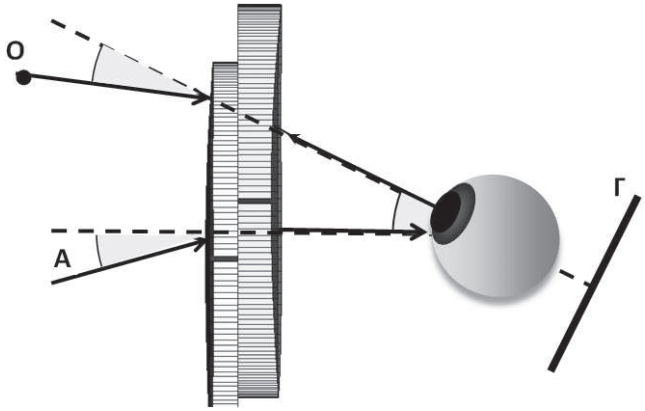

Figure 1. General scheme to compute power error and astigmatism for different gaze directions.

candidate to model progressive addition lenses (PALs). While PALs are, in general, free-form surfaces and thus are not amenable to explicit analysis, the Alvarez lens has a simple analytical form. To see this property of the Alvarez surface, consider a wavefront propagating in air and then refracted by a lens surface $u(x, y)$ into a lens with refraction index n. In the paraxial limit, where we neglect the effect of ray refraction (i.e. the normal to the wavefront and the normal to the refraction surface are nearly the same), the power (i.e. curvature) of the refracted wavefront is given by [20]

$$P_a = \frac{n-1}{2}(u_{xx} + u_{yy}). \tag{4}$$

Applying this formula to the surface (1) gives

$$P_a = 2(n-1)Ax. \tag{5}$$

This property of varying power is of course undesired when designing a single vision lens, where one prefers a lens with stable optical power. Thus we term the power deviation at any given point from the power at the lens center: power error. It seems at first sight that an optical element like the one we consider here, where the element consists of two Alvarez-type surfaces with essentially the same Alvarez coefficient A, will have a negligible power error. Indeed, let $Q_1 = (x_1, y_1, u_1(x_1, y_1))$ and $Q_2 = (x_2, y_2, u_2(x_2, y_2))$ be the hit points of the wavefront with the front and back surfaces, respectively. Let u_1 and u_2 both be of the same shape (1) except that one of them is shifted vertically by some distance $T = u_1(0, 0) - u_2(0, 0)$. We assume again the paraxial limit (4), and furthermore we use a thin lens approximation, where the length traveled by the wavefront inside the lens is negligible relative to its radius of curvature. Then, after refraction at the front and the back surface the power of the wavefront is

$$P_a = 2(n-1)A(x_1 - x_2). \tag{6}$$

Finally, the paraxial and thin lens approximations together imply that $x_1 \sim x_2$, and thus $P_a \sim 0$.

It turns out, however, that the calculation above is not valid for a typical Alvarez pair in a practical setup. The reason is that the cubic growth of the surfaces, and the constraints it imposes on the thickness at the lens vertex and near the frame, imply that the thin lens approximation is not precise enough in the sense that the deflection $x_1 - x_2$ is not negligible. For example, we calculated a practical design where our goal was to achieve an Alvarez lens with 5 D dynamic range with lateral shifts of up to 1 mm. This required us to select the Alvarez coefficient $A = 0.00125$. For such a lens we found out that, using a reasonable central thickness, a ray in a gaze direction of about 20° along the horizontal ($y = 0$ axis) is shifted in the x direction by at least 1 mm, that is $x_1 - x_2 > 1$. Using formula (6) with $n = 1.5$ implies that the power of such a wavefront is over 1.25 D in this moderate gaze direction. Since the power at the vertex is zero, we obtain a power error of at least 1.25 D. The rough calculation above was verified by us using the precise tracing algorithms mentioned in section 2.1.

We thus conclude that even an optical element consisting of two identical Alvarez surfaces suffers from a considerable power error. One possible way to reduce the power error is to apply a mechanical design that allows for a larger relative shift, thus enabling the reduction of the coefficient A without compromising the dynamical range of the lens. However, we note that larger lateral shifts also increase power errors, so a full optical design methodology must always be applied, such as the one presented in section 3.

2.3. Prismatic errors

Besides optical aberrations, prismatic errors are also considered in ophthalmic lens design. In conventional spectacles, these errors appear in the presence of lens misalignments (e.g. pantoscopic or dihedral tilts) with respect to the line of sight [15]. However, in Alvarez lenses prismatic errors are present even without misalignments [11].

Consider an Alvarez surface of the form $u(x, y) = Ax^3/3 + Cx$, so $\partial_x u = Ax^2 + C$. This implies that the normal at the vertex point of the surface $u(0, 0)$ is not collinear with the optical axis (z-direction), unless $C = 0$. Hence the chief ray traced along the optical axis is deflected from it after refraction at the Alvarez lens. Of course it is possible to select the parameter C in order to cancel (or minimize) the prismatic error, but when a lateral shift between the lenses is introduced this cancelation is lost (angle A in figure 1 cannot be zero at the same time for all focus configurations). For illustrative purposes we show an example of this effect in figure 2. A simple Alvarez lens was found to cancel the prismatic error for the neutral configuration (no lateral shift between lenses). However, when the lenses are moved to generate positive power (figure 2(a)) the chief ray is deflected in the $-x$ direction. Conversely, if lenses are moved to generate negative power (figure 2(b)) the chief ray is deflected in the opposite direction.

As an alternative, we propose a simple way to partially minimize the effects of prismatic errors. First, one should minimize the prismatic error only for the neutral configuration by means of including it as a target in the optimization merit function used to design Alvarez lenses. In a second stage, one can apply a strategy, already used in ophthalmic

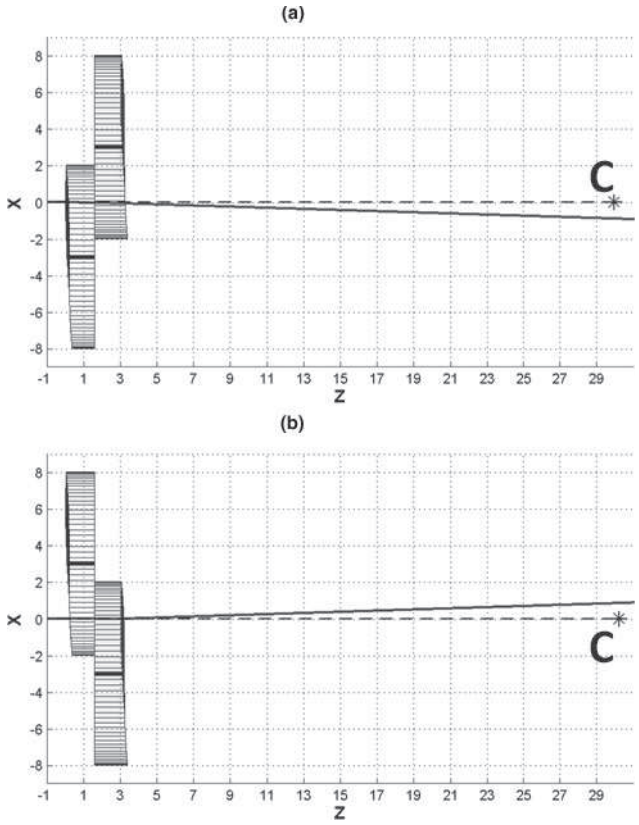

Figure 2. Chief ray tracing (black solid line) through shifted Alvarez lenses inducing (a) positive power or (b) negative power. C is the center of rotation of the eye.

lens design, to attenuate the pantoscopic angle [21]: the two lenses can be moved by the same magnitude ($+x$ direction in figure 2(a) and $-x$ direction in figure 2(b)) such that the chief ray passes through the center of rotation of the eye (C in figure 2). Obviously, for this purpose it is necessary to design a mechanical frame that can move each lens independently, like the one proposed in our previous work [10].

2.4. Merit function

In a zoom system the optical quality is typically controlled for three different focus positions [22]. Similarly, we optimized the optical quality of our lens for three relative positions between lenses, denoted by the index j: both lenses are shifted by $-\Delta$ mm ($j = 1$), lenses are not moved ($j = 2$), and lenses are shifted by $+\Delta$ mm ($j = 3$). Here Δ is the maximal lateral shift between lenses. We define the following variables:

- PC_j is the target power at the center of the lens for each configuration j (relative position between lenses).
- The index i denotes a point on the lens surface, determined by the gaze direction.
- P_{ji} and A_{ji} are, respectively, the power and astigmatism for a specific point i on the lens for a specific lens configuration j. From here we define the power error as $\mathrm{PE}_{ji} = |P_{ji} - \mathrm{PC}_j|$.
- The variable PR_2 is the prismatic deviation at the center of the lens for the neutral configuration $j = 2$. The prismatic error PRE is defined as $\mathrm{PRE} = |\mathrm{PR}_2|$.
- An important term in the merit function controls the power variation upon a lens shift. We call it central power error, and define it as $\mathrm{CPE} = |P_{1I} - \mathrm{PC}_1| + |P_{3I} - \mathrm{PC}_3|$, where P_{1I} and P_{3I} are the computed central power and PC_1 and PC_3 are the target nominal central powers for lens configurations $j = 1$ and $j = 3$, respectively.
- It is useful to weigh the power and astigmatism of each lens in each configuration with respect to the viewing directions. Therefore we define two weighted functions; weighted power WPE and weighted astigmatism WA:

$$\mathrm{WPE} = \frac{\sum_{j=1}^{j=3}\sum_{i=1}^{i=n} \mathrm{wp}_{ji}\mathrm{PE}_{ji}}{3n}, \tag{7}$$

$$\mathrm{WA} = \frac{\sum_{j=1}^{j=3}\sum_{i=1}^{i=n} \mathrm{wa}_{ji}|Aji|}{3n}. \tag{8}$$

Here we used wp_{ji} and wa_{ji} to denote the weights of the power error and astigmatism error, respectively.

Using the variables defined above, we set the merit function to be

$$\mathrm{MF}_1 = \mathrm{WPE} + WA + w_\mathrm{r}\mathrm{PRE} + w_\mathrm{c}\mathrm{CPE}, \tag{9}$$

where w_r and w_c are relative weights. We also defined an auxiliary merit function, that will be used in the optimization process:

$$\mathrm{MF}_2 = |P_{2I} - \mathrm{PC}_2|. \tag{10}$$

2.5. Optimization strategy

We optimized the merit functions with the Nelder–Nead algorithm as implemented in the MATLAB optimization toolbox, though with some slight variations, specifically the way the initial simplex is constructed.

The optimization of the merit function is performed with respect to many parameters (the nine parameters of equation (3)) for each surface of the Alvarez lens. To define an efficient optimization process one can adapt a cascade approach, where different design parameters are optimized at successive steps. At each step, the initial values used to start the new optimization are the values of the parameters obtained at the previous step.

We used the procedure shown in the flow chart of figure 3. The rectangular boxes show the parameters optimized at each step, and MF_i denotes the merit function used at each step. The superscript denotes whether the parameter refers to the posterior (2) or the anterior lens (1). R, Q and p_j are the different parameters of equation (3).

In a first step, the optimization procedure selects the initial values for the radii of curvature. An initial value for R^1 is chosen, and then the value R^2 that minimizes the merit function MF_2 is calculated. From this first optimization, the subsequent steps minimize the global merit function MF_1.

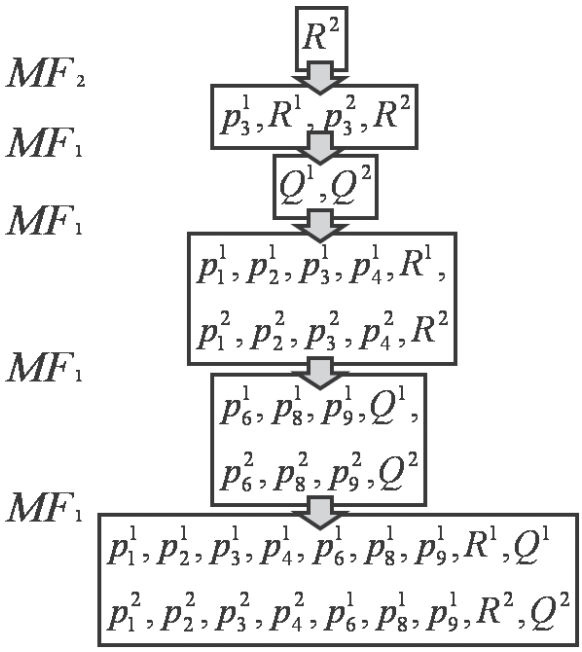

Figure 3. Flow chart in the optimization algorithm. Rectangular boxes contain the parameters optimized at each step. MF_i denotes the merit function used at each step.

2.6. Automatic weight adjustment

In optical design, when different quality metrics are targeted simultaneously, proper selection of the weights assigned to each target is critical for a successful optimization. It has been recognized that the weights must be large enough to force reduction of the specific associated errors but, at the same time, their values should not be too large, because they could distort the merit function topology, thus breaking the correspondence between its minimization and finding an optimal design [25].

Typically, optical designers set fixed weights for the optimization, but in many cases they have to manually adjust the weights after some optimization iterations in order to obtain better results. One way to avoid this trial and error step is to select a method that automatically determines weight adjustments in each iteration [23, 24]. This type of approach is particularly suitable when cost-based tolerances are included in the merit function [23].

Following this idea we applied a novel weight adjustment algorithm suitable for our design problem. We considered that power errors or astigmatism below 0.25 D are inside the acceptable tolerance in spectacle lens design. Therefore, if PE_{ji} or A_{ji} takes values below 0.25 D during the optimization process, the algorithm sets the weights wp_{ji} or wa_{ji} to zero. If the values exceed 0.25 D then the weights are set to be

$$\mathrm{wp}_{ji} = \frac{|\mathrm{PE}_{ji}|}{\max\{\mathrm{PE}_{ji}\}} \qquad \mathrm{wa}_{ji} = \frac{|A_{ji}|}{\max\{A_{ji}\}}. \tag{11}$$

3. Example of application of the optical design methodology

To show the potentials of our design methodology we present an example of a lens design for myopia correction. To increase the range of adjustable power, the quantity p_1 (see equation (3)) must also increase. However, it is not practical to seek a design of adjustable spectacles covering the whole range of refractive power errors because of physical dimension and optical performance requirements. Therefore we shall present a design that can correct myopia for a large subset of the population.

To find a reasonable range of refractive errors, we examined two sets of data on refractive error prevalence. One such study is based on the USA 1999–2004 National Health and Nutrition Examination Survey [26], and the other study covers Chinese people in Singapore [27]. Myopia was defined [27] as a refraction worse than −0.5 D, and high myopia as a refraction worse than −5 D. In the USA study, the prevalence of myopia was 44.7%, out of whom 14.5% were high myopic, whereas in the Singapore study the proportion of high myopes over the total amount of myopes was slightly larger (20%), though some of these differences could be attributed to differences in the average age of the populations used in these studies [26]. Considering these data, a minus spectacle model with a power variation from −0.5 to −5 D could serve the majority of the myopic population. A second minus model ranging from −5 to −10 D could serve almost all high myopes.

We designed a lens with a power variation from −0.5 to −5 D. The dynamical range of 4.5 D was obtained using a maximal lateral shift of 3 mm. We comment that the selection of 3 mm is, at this stage, arbitrary. The maximal lateral shift is an *a priori* design parameter that depends on several criteria. On the one hand, a large maximal lateral shift permits reducing the quantity p_1 to achieve a specific power variation and, as a consequence, to reduce the 'surface aberrations' of the Alvarez lens and the axial dimensions of the spectacles. On the other hand, smaller maximal lateral shift implies smaller lateral dimensions, but higher p_1 quantities. Also, a setup of small lateral shifts inducing large power changes would imply that unwanted misalignments of the lenses could generate noticeable aberrations.

3.1. Pre-design

The initial lens of the pre-design was obtained by applying the first two steps represented in the flow chart shown in figure 3. In the first step, the optimization procedure selects the initial values for the radii of curvature. Starting from an initial value for the radius of the anterior lens, the value of the posterior lens radius is obtained by setting the power at the central position for the neutral configuration (optimizing merit function MF2). In the second step, the parameters directly contributing to the central power are optimized (p_3 and R) using the merit function MF1.

The surfaces, of the form of equation (3), had the following values for the coefficients: inner lens,

$$[c, K, p] = [1/99.73, 0, 0.000\,117, 0, 0.000352, 0, 0, -0.016, 0], \tag{12}$$

and outer lens,

$$[c, K, p] = [1/186.72, 0, 0.000\,117, 0, 0.000352, 0, 0, -0.016, 0]. \tag{13}$$

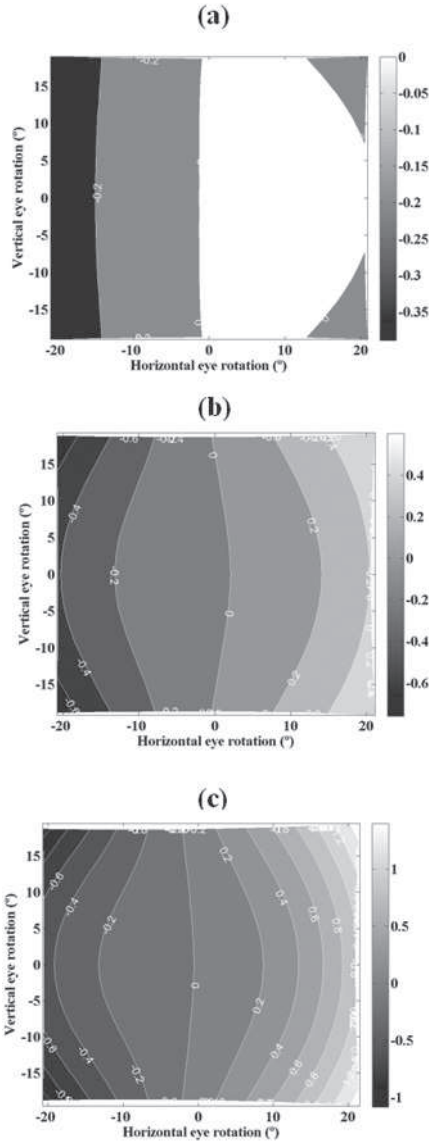

Figure 4. Power error (D), power deviation from the value at the center, for the pre-design lens at three different shift-locations, corresponding to three different central powers: (a) −0.49 D, (b) −2.77 D and (c) −4.99 D. The x–y axes are the horizontal and vertical eye rotations.

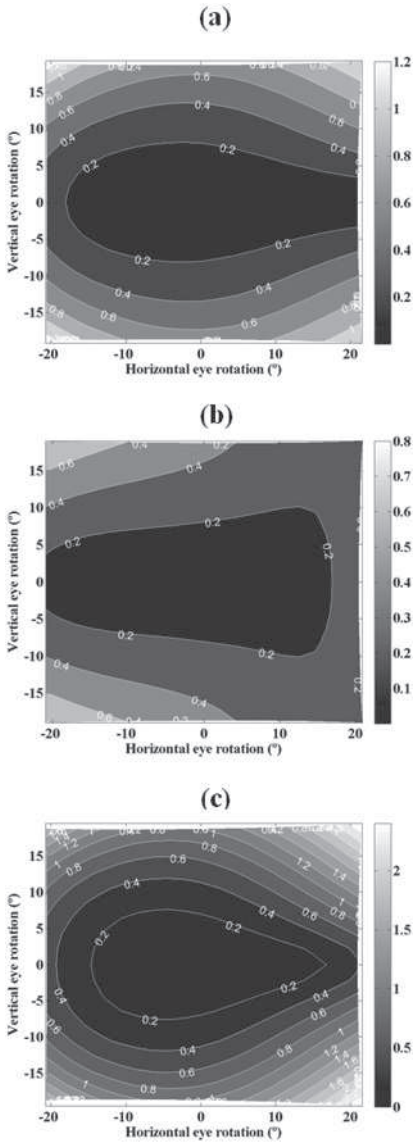

Figure 5. Astigmatism (D) for the non-optimized lenses at three different shift-locations, corresponding to three different central powers: (a) −0.49 D (b) −2.77 D and (c) −4.99 D. The x–y axes are the horizontal and vertical eye rotations.

It was assumed that the refraction index is 1.586 (polycarbonate).

The optical analysis was performed for a region covered by 20° × 18° of eye rotations (gaze directions). We computed the power error distribution (figure 4), namely the power deviation from the value at the center, and the astigmatism (figure 5) of the initial lenses defined above for three different shifts: both lenses are shifted by 3 mm (in opposite directions) to provide less negative power (figures 4(a) and 5(a)), lenses are not moved (figures 4(b) and 5(b)) and both lenses are shifted by −3 mm to provide more negative power (figures 4(a)–(c) and 5(c)). The central powers for the first and third shift-locations are −4.99 D and −0.49 D, respectively.

We observe that the absolute value of the power error is around 0.4 D for many gaze directions, in particular for the more negative power configuration (figure 4(c)). The astigmatism is comparable to the power variation, although it is sometimes larger, and at some points was found to be as high as 1 D.

3.2. Optimized design

Applying our optimization method to the above pre-design we obtained the following optimal parameters.

$$[c, K, p] = [1/100.4, 1.8 \times 10^{-5}, 0.000\,12, 4.16 \times 10^{-6}, 0.000\,36, 6.95 \times 10^{-6}, 5 \times 10^{-5}, -0.016, 2.96 \times 10^{-6}] \quad (14)$$

for the inner lens and

$$[c, K, p] = [1/189.53, 9.33 \times 10^{-5}, 9.92 \times 10^{-5}, 3.63 \times 10^{-6}, 0.000\,29, 6.03 \times 10^{-6}, 2.96 \times 10^{-6}, -0.0161, 2.96 \times 10^{-6}] \quad (15)$$

for the outer lens.

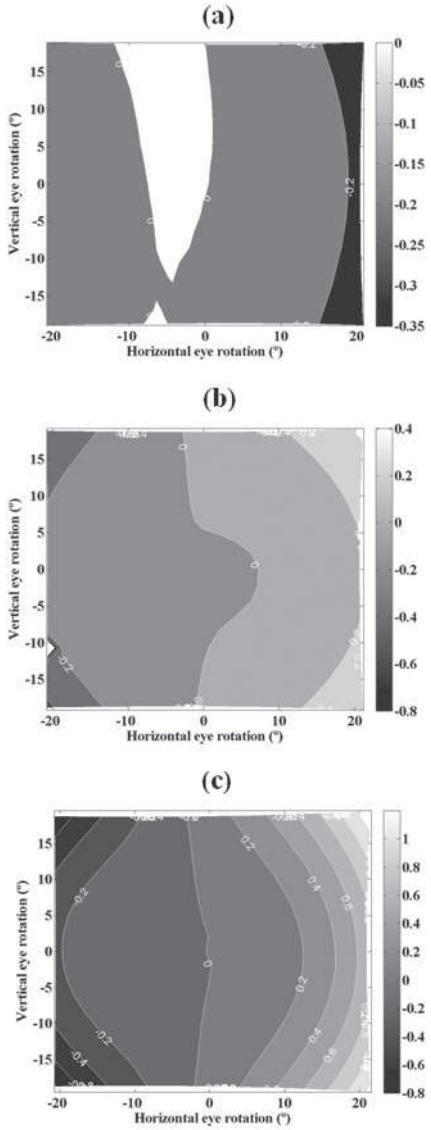

Figure 6. Power error (D), power deviation from the value at the center, for the pre-design lens at three different shift-locations, corresponding to three different central powers: (a) −0.53 D, (b) −2.82 D and (c) −5.04 D. The x–y axes are the horizontal and vertical eye rotations.

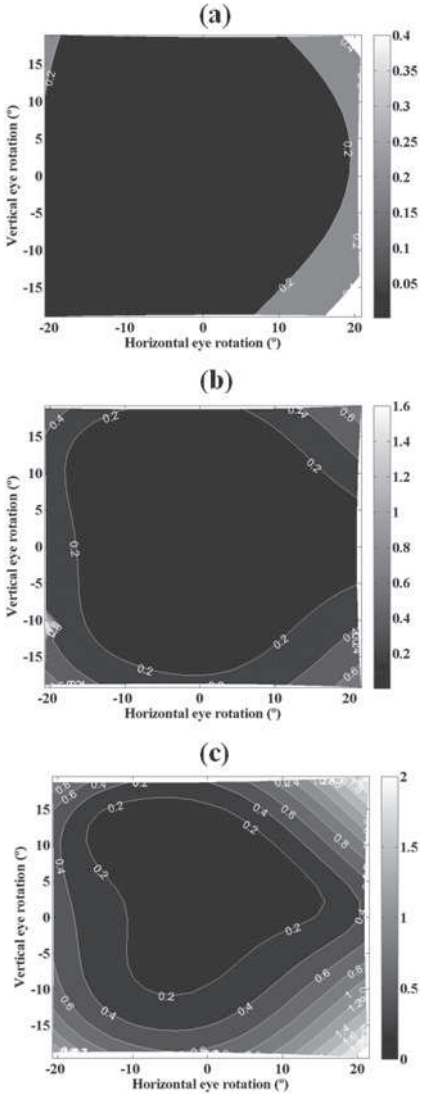

Figure 7. Astigmatism (D) for the optimized lenses at three different shift-locations, corresponding to three different central powers: (a) −0.53 D, (b) −2.82 D and (c) −5.04 D. The x–y axes are the horizontal and vertical eye rotations.

In figures 6 and 7 we depict the power variation and the astigmatism for the optimized lens. We observe that the absolute value of the power error and astigmatism is now under 0.2 D for most of the optical zone under consideration. Comparing to figures 4 and 5 we see that the power error and the unwanted astigmatism were reduced by a factor of at least 2.

4. Mechanical design

The need to reduce the lens thickness because of anatomical and mechanical constraints was already realized by Alvarez himself. He proposed [1] to add a linear function cx to the monkey saddle surface. Following this idea, Barbero [11] derived a formula for the linear coefficient, as a function of the lens diameter and the cubic coefficient, that optimally reduces the overall thickness.

However, such a procedure has two drawbacks. First, the linear coefficient that optimally reduces thickness is not necessarily optimal in terms of overall optical quality of the lens. Second, as we shall see shortly, this procedure may not suffice to achieve a sufficient thickness reduction at some parts of the lens.

In addition, for any type of spectacle frame on which the lens is mounted, the edge thickness has restrictions depending upon the frame design. As an example, a spectacle lens frame has been presented [10] where the edge thickness only admits variations from 1.5 to 2.4 mm. Even with a rimless spectacle frame the edge thickness must be controlled. For example, extremely large edge thickness, besides having aesthetically unpleasant appearance, could cause the eyelids to touch the lens.

We therefore divided the lens into two areas. The inner area is the optical zone that was optimized in section 3.2. The

outer area of the lens is the mechanical zone that connects the optical zone to the frame. The surface in the mechanical zone is given by an auxiliary analytical function that is derived by certain conditions on the smoothness of the combined surface, and by the constraints imposed by the frame structure.

We first describe the conditions that the auxiliary analytical surface in the mechanical zone must satisfy, and how to construct this zone in a lens with a circular shape. We then extend the derivation of the mechanical surface for a non-circular contour used in spectacle frames. The different constructions are demonstrated via examples.

4.1. Circular lens contours

The optometric industry typically uses lenses with circular shape. We therefore start by constructing the mechanical surface for such a case. It is convenient to use here polar coordinates. Denote the optical (generalized Alvarez) surface by $u(r, \theta)$ and the mechanical surface by $w(r, \theta)$. Let R_0 be the lens total radius, and let $r = R$ be the boundary between the optical and mechanical zones.

The function $w(R_0, \theta)$ sets the thickness at the edge. In addition, some continuity of the overall surface at the boundary contour is desired. One reason for the desired smoothness is optical, as strong discontinuities would imply local irregularities of the wavefront propagation at the boundary, or even scattering effects. Yet another reason is aesthetic; surfaces discontinuities are noticed by other observers, which makes the wearer less appealing. Indeed this problem becomes apparent by visual inspection of some models that are now present on the market.

Considering these issues, our goal is to find an analytical expression for $w(r, \theta)$ satisfying the following three conditions:

Continuity: $u(r, \theta)$ and $w(r, \theta)$ are equal at $r = R$.

Smoothness: the junction of $u(r, \theta)$ and $w(r, \theta)$ is smooth in the sense that the first and second radial derivatives are equal at $r = R$.

Edge behavior: the edge thickness of $w(R_0, \theta)$ is a prescribed function $e(\theta)$.

It is convenient to express $w(r, \theta)$ in the form

$$w(r, \theta) = a_1(\theta) + a_2(\theta)(r - R) + a_3(\theta)(r - R)^2 + a_4(\theta)(r - R)^3. \quad (16)$$

The four conditions mentioned above are represented by the following four equations:

$$a_1(\theta) = u_{r=R}, \quad (17)$$

$$a_2(\theta) = \partial_r u_{r=R}, \quad (18)$$

$$2a_3(\theta) = \partial_{rr} u_{r=R}, \quad (19)$$

$$a_1(\theta) + a_2(\theta)(R_0 - R) + a_3(\theta)(R_0 - R)^2 + a_4(\theta)(R_0 - R)^3 = e(\theta). \quad (20)$$

Equations (17)–(19) directly provide explicit expressions for $a_1(\theta)$, $a_2(\theta)$ and $a_3(\theta)$. Then we can compute $a_4(\theta)$ by direct substitution in equation (20):

$$a_4(\theta) = \frac{e(\theta) - a_1(\theta) - a_2(\theta)(R_0 - R) - a_3(\theta)(R_0 - R)^2}{(R_0 - R)^3}. \quad (21)$$

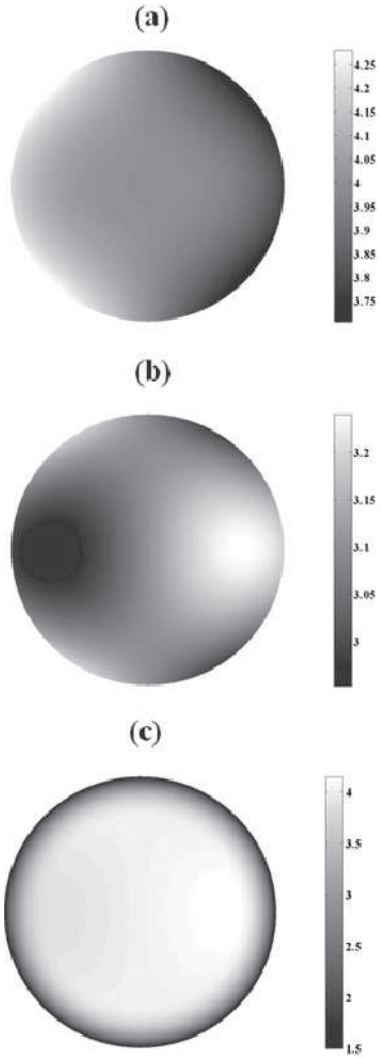

Figure 8. Lens thickness (mm) distribution inside a circular area of pupil radius of 15 mm for lens examples A, B and C respectively.

As an example of the mechanical zone construction, we define three lenses. First, the lens (A) with the surface represented by equation (3), where the linear term is set to zero $p_6 = 0$, second (lens B) where we applied a thickness reduction using the optimal value of $p_8 = -0.0161$ as computed in [11]. Figure 8(a) shows the lens thickness distribution inside the lens for the first case and figure 8(b) for the second case. Figure 9 shows the edge thickness as a function of the angular coordinate. It is easily seen how the linear term reduced the thickness variations of the original monkey saddle surface, but the edge thickness is not uniform, ranging from 2.9 to 3.1 mm, which would make this lens not suitable for the frame proposed in [10].

In the third lens (C) we applied the mechanical zone construction as explained above. The optical zone was set to be $R = 8$ mm. The edge thickness was selected as $e(r = R_0, \theta) = 1.5$ mm, with $R_0 = 12$ mm. Figures 8(c) and 9 show the lens thickness distribution for this case. In the new construction (lens C) we have a uniform thickness distribution at the edge, and the constant thickness is within the limitation imposed by the frame mechanics, unlike lenses A and B.

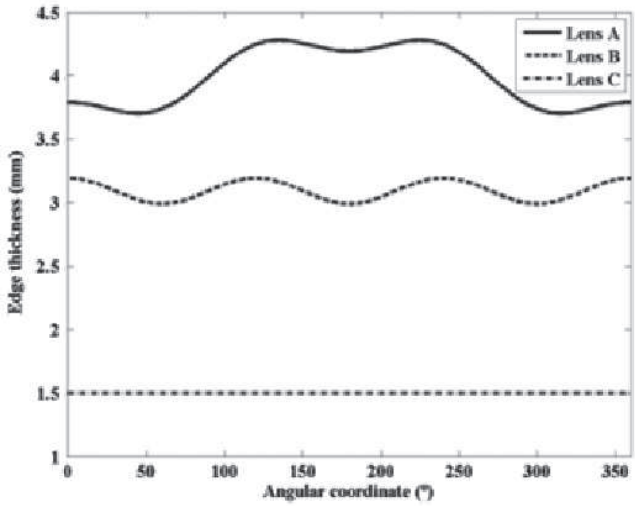

Figure 9. Edge thickness (mm), thickness along the circular contour, for lens examples A, B and C.

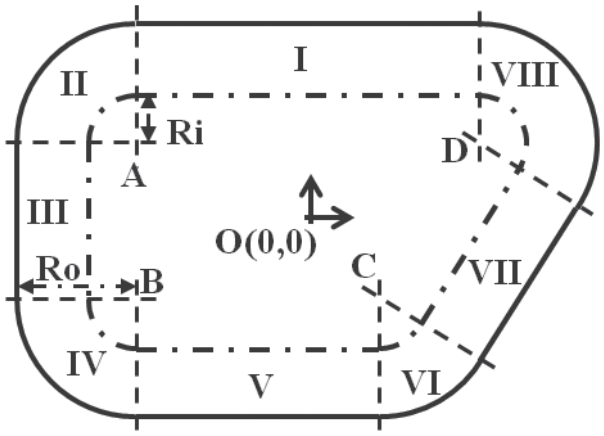

Figure 10. Geometry construction of a general lens contour. Zones I–VIII represent the mechanical zone.

4.2. General lens contours

There is a great diversity of eyeglass frame shapes: square, rectangular, oval, etc [21]. A generic shape, shown in figure 10, comprises of rectilinear edges with rounded corners. The rounded corners are circular arcs of specific radii of curvature. The frame width decreases downwards at the nasal area following the increase of the nose width. The boxed lens system is used to define the lens shape [21]. A rectangle is formed by the horizontal and vertical tangents to the lens contour [15]. The boxed lens size is the dimensions of this rectangle and the boxed center is the geometrical center of the rectangle [21].

The lens edge shape of figure 10 can be described by the coordinates of five points. The optical center of the lens is the point O, which might coincide with the boxed center or not. It is set to be the center of coordinates. The additional four points

$$\mathrm{A} = (x_a, y_a), \qquad \mathrm{B} = (x_b, y_b),$$

$$\mathrm{C} = (x_c, y_c), \qquad \mathrm{D} = (x_d, y_d)$$

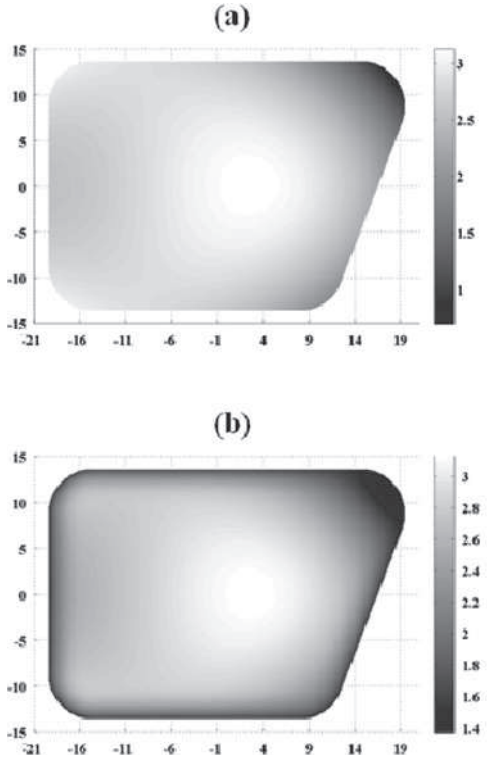

Figure 11. Lens thickness (mm) distribution with surface represented by equation (14). (a) No mechanical zone construction. (b) Mechanical zone construction inside the non-circular geometry represented in figure 10, where A = (−14.5, 8.7), B = (−14.5, −8.7), C = (7.86, −8.7), D = (8.7, −8.7), $R_o = 5$ mm, $R_i = 0.5$ mm.

are the centers of curvature of the circular arcs of the edge corners.

We observed that for non-circular frame shapes it is preferred to use a frame-dependent mechanical zone over a circular mechanical zone construction, because a frame-dependent zone provides smoother surfaces. Therefore, in the present design we define the boundary separating the optical zone and the mechanical zone as the offset shape of the frame contour. Exploiting the particular geometry of the frame, this offset is created by defining a different circle radius for the corners. As shown in figure 10, for the inner contour we select the radius R_i and for the outer curve (frame contour) we select R_o.

Using the base points (A, B, C, D) we divide the mechanical zone into eight compartments as depicted in figure 10. We derived analytical expressions for these compartments. It is then straightforward, although algebraically involved, to construct a surface defined over each compartment, so that the combined lens surface meets all the smoothness requirements, that is, it is twice differentiable at the boundary curve, and also meets the desired shape at the frame contour.

As in section 4.1, we demonstrate via an example the benefits of controlling the thickness for this general contour using the auxiliary surface construction. Figures 11(a) and (b) show the lens thickness distribution of the surface represented by equation (14) without and with the mechanical zone

construction, respectively. The coordinates of the points defining the lens contour were

$$A = (-14.5, 8.7), \qquad B = (-14.5, -8.7),$$

$$C = (7.86, -8.7), \qquad D = (8.7, -8.7).$$

The corners' circle radius was set to 5 mm and the corners' circle radius defining the inner contour to 0.5 mm. As before, the edge thickness was selected as $e(r = R_o, \theta) = 1.5$ mm.

5. Discussion

We have presented a comprehensive approach for the design of an adjustable-focus lens based on the Alvarez principle. Our design consists of dividing the lens into two parts, an optical zone and a mechanical zone.

For the optical part we presented a design methodology to optimize the optical performance of the lens for different lateral shifts and for different gaze directions. The methodology involves a cascade of optimization steps. An important novelty of our design methodology is that the optimized lenses of the Alvarez pair are not equal, which is due to the fact that the thin lens approximation is not appropriate for these designs, as shown in section 2.2.

As an example we showed that a pair of lenses of reasonable optical quality can be obtained with a power dynamical range of 4.5 D with just ±3 mm lateral shift. The lenses designed with our optical design methodology can be manufactured using plastic injection molding, thus ensuring a low-cost technology. The mold could be manufactured with the help of a single point diamond turning machine.

While our design methodology has demonstrated the feasibility of designing adjustable-focus lens with suitable power dynamical range and reasonable optics, we now discuss some possible ways to improve the design.

First, it could be possible to use more complex surfaces, such as free-form surfaces, instead of the surface equation (3). Still, it would be convenient to apply the design outlined above as a starting point in an iterative algorithm modifying the local parameters describing the free-form surface.

We pointed out in section 2.1 that in conventional ophthalmic lens design the pupil size is ignored, and therefore the pupil aberrations such as coma were not analyzed by us. This is a reasonable assumption for simple lenses. However, for lenses comprising complex surfaces, such as PALs, higher order aberrations are now being considered [28, 20]. This could be also done for Alvarez lenses. In the same context we comment that equation (3) can be expressed in terms of normalized Zernike polynomials (specifically coma, trefoil, tilt, and defocus). This representation could shed light on the 'surface aberrations' introduced by Alvarez lenses, including coma. However, full ray tracing must be performed because, as explained before, the paraxial approximation is not good enough for thick Alvarez lenses.

Regarding the mechanical zone, we showed how to construct a mechanical zone of the lens to connect the optical zone with the frame. Such a zone is needed since it is hard to design a large optical zone and because the Alvarez principle implies a rapid growth of the lens thickness. Our construction of the mechanical zone guarantees a smooth overall surface, since at the boundary between the zones the surfaces are by definition twice continuously differentiable.

We have presented two methods for two particular frame designs. A similar construction can be done for arbitrary frame contour by using an appropriate local coordinate system. In some extreme cases of edge thickness function e we observed that the strong smoothness assumption at the boundary curve gives rise to inflection points in the resulting surface. This can be prevented by relaxing the smoothness condition, for example by requiring only continuity of one derivative normal to the boundary curve. Another option is to define the surface in the mechanical zone by solving a Willmore–Helfrich type minimization problem [29] with appropriate boundary conditions.

We are now continuing our work along the lines we just described for both the optical and mechanical components of the lens. We are also exploring new concepts for the frame design.

References

[1] Alvarez L W 1967 Two-element variable-power spherical lens *US Patent* 3,305,294

[2] Lohmann A W 1970 A new class of varifocal lenses *Appl. Opt.* **9** 1669–71

[3] Resnikoff S, Pascolini D, Mariotti S P and Pokharel G P 2008 Global magnitude of visual impairment caused by uncorrected refractive errors in 2004 *Bull. World Health Org.* **86** 63–70

[4] Holden B A, Fricke T R, Ho S M, Wong R, Schlenther G, Cronje S, Burnett A, Papas E, Naidoo K and Frick K 2008 Global vision impairment due to uncorrected presbyopia *Arch. Ophthalmol.* **126** 1731–9

[5] Focus on vision www.focus-on-vision.org

[6] Eyejusters www.eyejusters.com

[7] AdLens http://adlens.com

[8] Van Asbeck F 2006 Combined lens and spectacles provided with at least one such combined lens *International patent* 2006/098618

[9] Van Der Heijde G L and Louwerse W P 2008 Glasses *International patent* 2008/002131

[10] Zapata A and Barbero S 2011 Mechanical design of a power-adjustable spectacle lens frame *J. Biomed. Opt.* **16** 055001

[11] Barbero S 2009 The Alvarez and Lohmann refractive lenses revisited *Opt. Express* **17** 9376–90

[12] Atchison D A 1985 Modern optical design assessment and spectacle lenses *Opt. Acta* **32** 607–34

[13] Tang C Y and Charman W N 1992 Effects of monochromatic and chromatic oblique aberrations on visual performance during spectcale lens wear *Ophthalmic. Physiol. Opt.* **12** 340–9

[14] Bourdoncle B, Chauveau J O and Mercier J L 1992 Traps in displaying optical performances of a progresive addition lenses *Appl. Opt.* **31** 3586–93

[15] Fowler C and Latham Petre K 2001 *Spectacle Lenses: Theory and Practice* (Oxford: Butterworth–Heinemann)

[16] Keller J B and Keller H B 1950 Determination of reflected and transmitted fields by geometrical optics *J. Opt. Soc. Am.* A **40** 48–52

[17] Kneisly J A 1964 Local curvature of wavefronts in optical system *J. Opt. Soc. Am.* A **54** 229–35

[18] Landgrave J E A and MoyaCessa J R 1996 Generalized Coddington equations in ophthalmic lens design *J. Opt. Soc. Am.* A **13** 1637–44

[19] Campbell C E 2006 Generalized Coddington equations found via an operator method *J. Opt. Soc. Am.* A **23** 1691–8
[20] Blendowske R, Villegas E A and Artal P 2006 An analytical model describing aberrations in the progression corridor of progressive addition lenses *Opt. Vis. Sci.* **83** 666–71
[21] Jalie M 2008 *Ophthalmic Lenses and Dispensing* (Edinburgh: Elsevier/Butterworth Heinemann)
[22] Malacara D, Malacara Z and Malacara D 2004 *Handbook of Optical Design* (New York: Dekker)
[23] Youngworth R N and Stone B D 2000 Cost-based tolerancing of optical systems *Appl. Opt.* **39** 4501–12
[24] Todd C D and Maxwell J 1996 Aberrational weight adjustment by tolerance based weighting in damped least squares optimisation *Design and Engineering of Optical Systems* ed J J M Braat, pp 89–105
[25] Vasiljevic D 2002 *Classical and Evolutionary Algorithms in the Optimization of Optical Systems* (Boston, MA: Kluwer Academic)
[26] Vitale S, Ellwein L, Cotch M F, Ferris F L and Sperduto R 2008 Prevalence of refractive error in the United States, 1999–2004 *Arch. Ophthalmol.* **126** 1111–9
[27] Wong T Y, Foster P J, Hee J, Ng T P, Tielsch J M, Chew S J, Johnson G J and Seah S K L 2000 Prevalence and risk factors for refractive errors in adult Chinese in Singapore *Invest. Ophthalmol. Vis. Sci.* **41** 2486–94
[28] Villegas E A and Artal P 2003 Spatially resolved wavefront aberrations of ophthalmic progressive-power lenses in normal viewing conditions *Opt. Vis. Sci.* **80** 106–14
[29] Helfrich W 1973 Elastic properties of lipid bilayers: theory and possible experiments *Z. Naturf.* **28** 693–703